LETTERS

Importance of rain evaporation and continental convection in the tropical water cycle

John Worden[1], David Noone[2], Kevin Bowman[1] & the Tropospheric Emission Spectrometer science team and data contributors*

Atmospheric moisture cycling is an important aspect of the Earth's climate system, yet the processes determining atmospheric humidity are poorly understood[1–4]. For example, direct evaporation of rain contributes significantly to the heat and moisture budgets of clouds[5], but few observations of these processes are available[6]. Similarly, the relative contributions to atmospheric moisture over land from local evaporation and humidity from oceanic sources are uncertain[3,7]. Lighter isotopes of water vapour preferentially evaporate whereas heavier isotopes preferentially condense[8–10] and the isotopic composition of ocean water is known. Here we use this information combined with global measurements of the isotopic composition of tropospheric water vapour from the Tropospheric Emission Spectrometer (TES) aboard the Aura spacecraft[11,12], to investigate aspects of the atmospheric hydrological cycle that are not well constrained by observations of precipitation or atmospheric vapour content. Our measurements of the isotopic composition of water vapour near tropical clouds suggest that rainfall evaporation contributes significantly to lower troposphere humidity, with typically 20% and up to 50% of rainfall evaporating near convective clouds. Over the tropical continents the isotopic signature of tropospheric water vapour differs significantly from that of precipitation[8,10,13], suggesting that convection of vapour from both oceanic sources and evapotranspiration are the dominant moisture sources. Our measurements allow an assessment of the intensity of the present hydrological cycle and will help identify any future changes as they occur.

Simultaneous profiles of HDO and H_2O are obtained from TES thermal infrared radiances between 1,200 and 1,350 cm^{-1} using maximum a posteriori optimal estimation[12] (Supplementary Information). This approach allows for a precise characterization of the errors in the ratio of singly deuterated water to water (HDO/H_2O) and its vertical resolution (see Supplementary Information). For this analysis, mean values of the isotopic composition (hereafter δD, see Methods) are calculated from averages of HDO and H_2O between 550 and 800 hPa, where the estimated profiles of δD are most sensitive. This average has a typical precision of 10‰ in the tropics and 24‰ at the poles[12]. Profiles of atmospheric and surface temperature, surface emissivity, an effective cloud optical depth and cloud top height are also estimated from TES radiances[14] and are used to stratify δD in analysis presented here. Global observations from 50 evenly distributed days between late October 2004 and March 2005 are used. There are 1,150 observations per day, of which typically 400 are found to be of suitable quality for this analysis[12]. The horizontal footprint of each observation is 8 km by 5 km.

A bias in the established HDO spectroscopic line strengths requires a correction of 5% in the estimated HDO profiles and is uniform across all observations. With this correction, the distribution of TES δD measurements is consistent with comparisons to theoretical modelling of infrared spectroscopic HDO line strengths, recent aircraft measurements, values expected near the ocean surface, and general circulation model simulations[12]. The bias correction accounts for the a priori constraint and vertical resolution of the HDO and H_2O profile retrieval (see Supplementary Information). Such a bias reduces the confidence one can place on absolute measures of hydrologic cycling derived from the data, but comparisons between different subsets avoid the impact of the bias on findings. For instance, the spatial distribution of observations shows a decrease of both water vapour amount and δD with higher latitudes that is robust irrespective of the bias (Fig. 1). This so-called 'latitude effect' is found also in measurements of δD of precipitation and is due to the preferential removal of heavier nuclides during condensation as vapour is transported poleward[8] and because rainfall tends to equilibrate isotopically to the background vapour as it falls[10,15,16].

TES δD vapour observations are plotted in Fig. 2a as a function of H_2O volume mixing ratio (q_{H_2O}) to distinguish evaporation from condensation processes and infer the water transport characteristics. Theoretical considerations give δD of vapour in equilibrium with ocean water, which is shown in Fig. 2 as the black line which spans sea surface temperatures from 5 to 25 °C. Bulk evaporation describes turbulent mixing of vapour from the saturated layer at the ocean surface into a drier air parcel aloft. The orange curves in Fig. 2 show the evolution of δD under continual evaporation towards isotopic composition of ocean sources of different temperatures. In contrast, a Rayleigh distillation model describes isotopic depletion as vapour is lost to precipitation. The cyan curves show Rayleigh predictions originating from a distribution of saturated oceanic vapour and assume a condensation temperature 15 K colder than the ocean surface (clouds at about 2.5 km). A simple description of the atmospheric water cycle is that any given observation of an air parcel will reflect a history of evaporation and Rayleigh condensation and therefore, as shown in Fig. 2a, lie between the theoretical extremes of the curve for condensation from moisture originating over a warm oceanic source and the curve for evaporation towards equilibrium with a cold oceanic source.

A Rayleigh paradigm posits moist air to be less depleted than dry air. This largely explains the extra-tropical oceanic observations seen in Figs 2b and 3, where moist observations (in which the relative humidity is larger than 80% and the cloud optical depth is larger than 0.3) are partitioned from dry and clear-sky observations (in which the relative humidity is less than 50% and cloud optical depth less than 0.1). Figure 2b shows that the evaporation curves more closely describe the dry air parcels while the Rayleigh condensation

[1]Jet Propulsion Laboratory, California Institute of Technology, Pasadena, California, USA. [2]Department of Atmospheric and Oceanic Sciences, and Cooperative Institute for Research in Environmental Sciences, University of Colorado, Boulder, Colorado, USA.
*A list of participants and affiliations appears at the end of the paper.

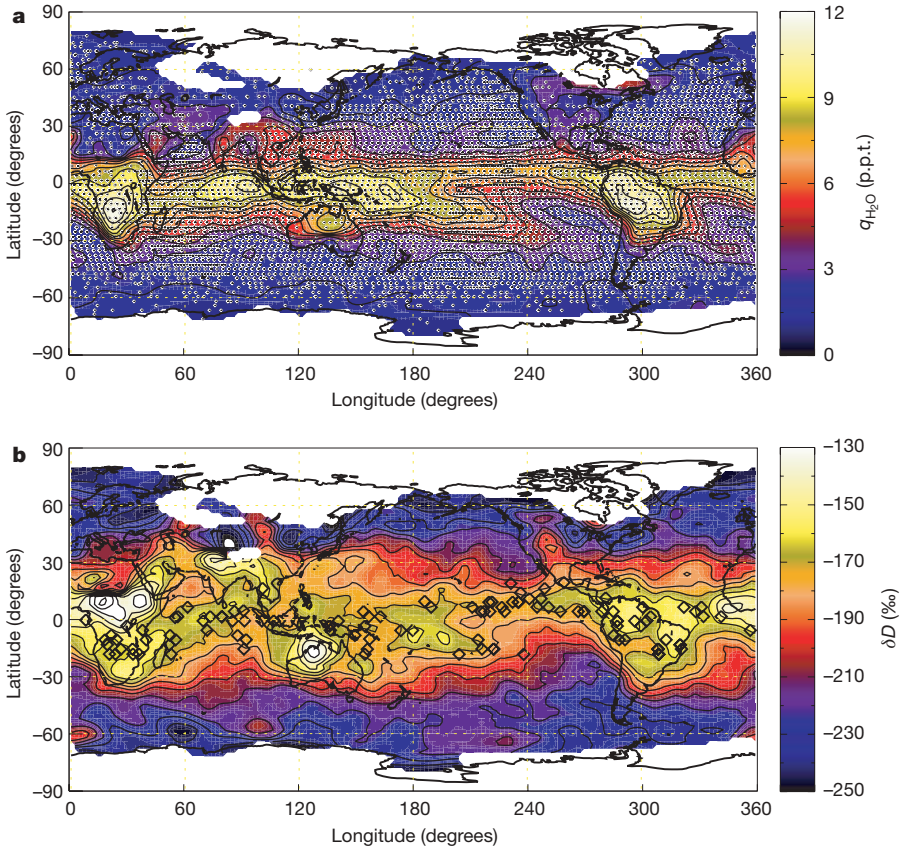

Figure 1 | Global distribution of TES observations averaged vertically between 550 and 800 hPa. **a**, Water vapour volume mixing ratio q_{H_2O} (parts per thousand by volume, p.p.t.). **b**, HDO (δD relative to VSMOW). Observations were made on 50 days between October 2004 and March 2005 at locations shown as dots in **a**. The data are gridded for plotting using a Cressman scheme with a mean effective radius of 500 km and a maximum radius of 1,200 km. The data are masked where there are less than two observations within 1,200 km. The diamonds in **b** show where the amount effect is evident.

curves more closely describe the moist air parcels. The difference between moist and dry air parcels is shown more clearly in Fig. 3. The extra-tropical dry air parcels are typically 16‰ more depleted than the moist air parcels. The standard error of the mean for the extra-tropics is approximately 2‰. The overlapping distributions are a reminder that any individual air parcel will have a history of both evaporation and condensation.

In sharp contrast to the extra-tropical observations, the tropical observations (Equator-ward of 20° latitude) are not described accurately by the Rayleigh description of evaporation from an oceanic source followed by condensation. Specifically, Fig. 3 shows moist tropical points are more depleted than dry tropical points by 12‰, with the standard error of the mean being 1‰. This excess depletion is also observed in Fig. 2c where individual observations show more depletion than do the set of possible Rayleigh curves. Over 99% of the clear tropical data lie within the two end-member models describing evaporation of a cold oceanic source at 5 °C and condensation from an oceanic source at 25 °C. However, over half of the tropical moist observations are more depleted than the Rayleigh condensation curve. A similar feature, termed the 'amount effect', is found statistically in monthly precipitation δD measurements in regions of intense rainfall and is often attributed to the evaporation of falling rain near active convection[8,17]. The TES vapour results confirm this rehydration mechanism by noting that the location of these anomalous observations corresponds to regions known for active convection (diamonds in Fig. 1b).

The role of rain evaporation can be understood by comparing vapour observations to values predicted by a bulk mass balance isotope model with differing rainfall evaporation fractions. The δD is modelled as an open system in which moisture gain via surface evaporation and advection from nearby is balanced by moisture loss via precipitation (Methods and Supplementary Information). In the model, some fraction of the rainfall is evaporated and returned to vapour, thereby producing the amount effect. Such balance is achieved only for adequately large regions in which the mean convective activity is in approximate quasi-equilibrium relative to the slowly evolving large-scale conditions[5,18,19]. The initial δD will vary with the rain evaporation fraction (that is, the vertical displacement of purple dots in Fig. 2c). Once the flux balance is broken, owing to changes in the advective, precipitation or evaporation rates, the net loss of water is accompanied by an isotopic evolution that follows a Rayleigh-like distillation (purple curves in Fig. 2c), and explains how moist tropical air parcels are more depleted than dry tropical air parcels. The steep slope results from the additional fractionation during rain evaporation and it is this which allows the final depletion to exceed that predicted from a Rayleigh model.

As indicated in Fig. 2c, very few observations require a modelled rain evaporation fraction in excess of 50%, whereas a fraction of around 20% passes through the centre of the distribution of cloudy observations. A mean rain evaporation fraction of 20% is estimated from our simple mass balance model (see Methods) by assuming that no rain evaporation has occurred in the history of the clear-sky observations and that the observed isotopic difference between cloudy and clear-sky observations is 12‰ (Fig. 3). This result is sensitive to the specific assumptions about isotopic exchange and the temperature of the ocean sources (here taken as 25 °C) but because this estimate of 20% is constrained by using the difference between the isotopic composition of the clear sky and cloudy observations (the red and blue curves in Fig. 3), and not their absolute amounts, it is not sensitive to the spectroscopic bias in the measurements. This

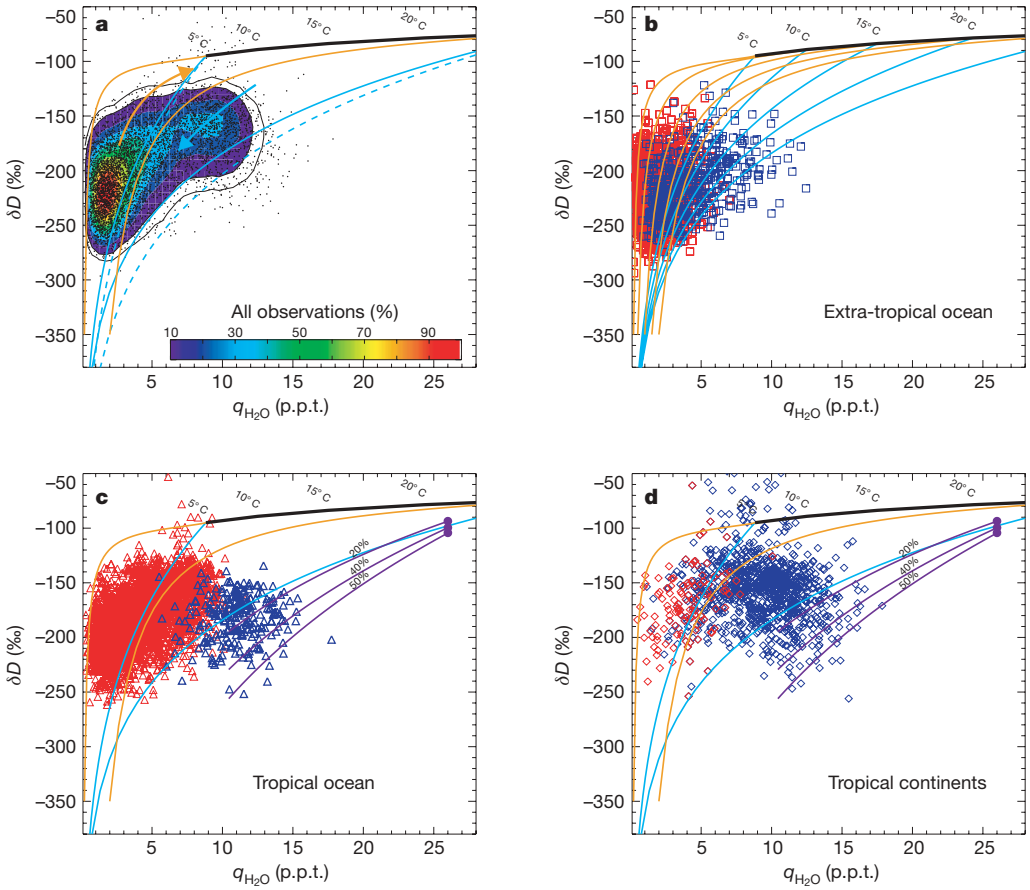

Figure 2 | Scatter plots of δ*D* versus q_{H_2O} reveal underlying hydrologic processes. a, Probability distribution of all data (colour shading shows the percentage of the most likely value; the outer black contour envelops 95% of the observations) with dots showing one in three observations. The orange, cyan and purple curves and the purple dots show model predictions as described in the Methods; they are derived in detail in the Supplementary Information. Observations are separated by location as follows: **b**, oceanic extra-tropics (poleward of 30°); **c**, oceanic tropics (Equatorward of 20°); and **d**, tropical continental areas. Observations are for clear-sky (optical depth < 0.2 and humidity < 50%, red symbols) and cloudy (optical depth > 0.3 and humidity > 80%, blue symbols) conditions. The solid black curve shows the isotopic composition of saturated vapour in equilibrium with the ocean water for a range of surface temperatures as marked in °C along the black line.

evaporation fraction estimate is consistent with the conservative estimate of 30% based on a radar study in a semi-arid environment[20] and values from climate model simulations[21]. More importantly, the isotopic distribution of moist and dry vapour as seen in Fig. 2c provides a new climatology with which to assess the cloud hydrology in climate and mesoscale models.

Comparison of the isotopic vapour over continents to that over ocean reveals a more complicated hydrologic cycle than is suggested by a simpler system in which condensation is balanced by evaporation. A conventional view inferred from isotopic measurements of continental precipitation is that an air mass becomes disconnected from the ocean source as it moves inland, and consequently the vapour and precipitation becomes more depleted further inland (the 'continental effect'[8,22]). In an apparently contradictory way, Fig. 3b shows that continental vapour observations are typically less depleted than the oceanic observations, especially over the Amazon and tropical Africa (Fig. 1b). In addition to these anomalous values, many tropical land observations also show an amount effect, in which the moist air parcels are more depleted than the dry air parcels. Consequently, the TES observations show that the conventional Raleigh description of a disconnected condensing air mass is inadequate for describing processes controlling free tropospheric water vapour over tropical land.

Two possible sources that can enrich the isotopic composition of free troposphere terrestrial vapour relative to the ocean merit attention—oceanic vapour transported at low altitude inland and vapour from evapotranspiration—both of which are then lofted into the free troposphere. There is a steep vertical gradient in the isotopic composition of water vapour[23,24], which follows the background thermal structure because of the integrated history of condensation. As such, air transported vertically by warm convection will be enriched relative to its surroundings. Vapour from evapotranspiration can be further enriched relative to the oceanic vapour because there is no net fractionation as soil water is extracted from the surface[13,25]. Evidence for this source is found in those observations that are enriched relative to oceanic vapour (that is, points above the black line in Fig. 2 are almost all cloudy tropical continental points). The amount effect also observed in the tropical land data occurs in regions that are seasonally moist (for example, South America, Southeast Asia). Vertical lofting of less-depleted vapour is found to dominate in arid regions where the convective cloud systems are expected to be characteristically different (for example, northern Australia, east Africa). The widely disparate sources and cloud processes over land highlight the need to account for the regional diversity in the balance of competing processes that affect tropical terrestrial hydrology.

Thus isotopic observations are powerful in diagnosing hydrologic processes that are otherwise not well measured but are central to understanding climate because they reflect exchange between water phases rather than the state measured by conventional (non-isotopic) quantities. Specifically, the isotopic distribution provides a metric for the intensity of the large-scale hydrological cycle through the balances between the rate at which the vapour is restored to known oceanic conditions by evaporation and boundary-layer mixing, and

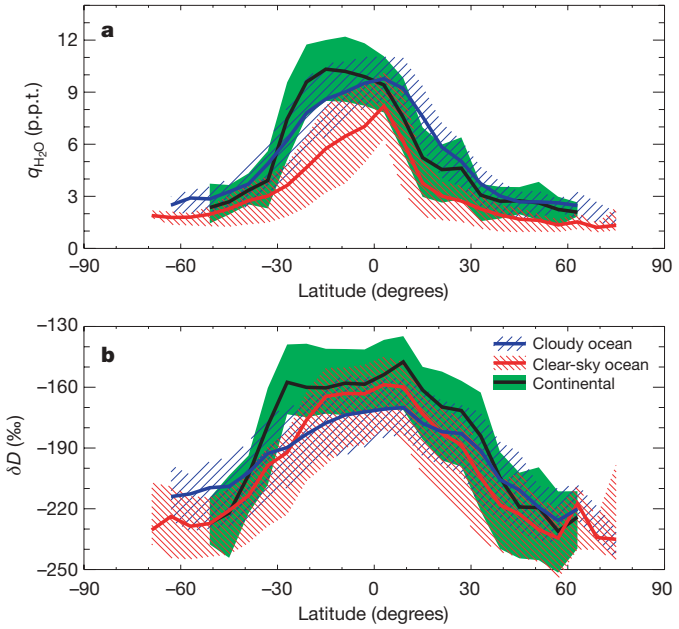

Figure 3 | Contrast between cloudy and clear sky ocean, and continental observations. Zonal mean observed water vapour q_{H_2O} (**a**) and δD binned at 6° latitude (**b**). The data are stratified (as in Fig. 2) to be clear-sky ocean (red, 53% of observations), and cloudy ocean (blue, 27% of observations). All land observations (black curve, green shading) represent 12% of observations. The red, blue and green shaded areas are bounded by the 25 and 75 percentiles of each subset. Errors on the means in **b** range between 1 to 2‰ for the data Equatorward of 50 degrees.

the rate at which water is removed by intermittent condensation events. Should the intensity of the hydrologic cycle change[4], isotopic assessment provides a framework for interpreting which processes and water sources are responsible.

METHODS

The isotope ratio is defined as $R = q_{HDO}/q_{H_2O}$, where q is the volume mixing ratio of HDO or H_2O. Isotopic composition is expressed as δD values, where:

$$\delta D = \left(\frac{R}{R_{VSMOW}} - 1\right) \times 1{,}000$$

R_{VSMOW} is the isotope ratio of Vienna Standard Mean Ocean Water reference (3.11×10^{-4}). All mean δD values are mass-weighted (that is, δD refers to mean q_{H_2O} and mean q_{HDO}). The foundation of isotopic analysis is that given adequate knowledge of the fractionation processes which accompany water exchange (evaporation, transport and precipitation), the history of the processes that acted on a distribution of observed air parcels can be inferred from δD. Conversely, should the behaviour of the water cycle be assumed, the details of the cloud physics can be deduced from their different effects on δD.

Isotope models shown as curves in Fig. 2 are derived from simple mass balance equations:

$$\frac{\partial q}{\partial t} = E - P + A$$

where A is the advection rate, E is the evaporation rate and P is the precipitation rate. P may be written as the difference between the total condensation rate, C, and the rainfall evaporation rate X (that is, $P = C - X$). Upon inserting expressions for isotopic fractionation during exchange processes, general equations governing the evolution of q_{HDO} and q_{H_2O} are written as the sum of three terms (see Supplementary Information for details):

$$\frac{\partial q_{H_2O}}{\partial t} = \gamma(q_s - q_{H_2O}) - (1-f)C + A$$

$$\frac{\partial q_{HDO}}{\partial t} = \gamma\eta(R_s q_s - q_{HDO}) - \alpha_c RC\left(1 - \frac{f}{\alpha_e}\right) + \overline{R}A$$

where γ is a bulk exchange coefficient for evaporation, q_s is the saturation mixing ratio at the ocean surface with isotopic composition in equilibrium with ocean water R_s, f is the fraction of rain evaporated, and $\overline{R}$ is the net isotopic composition of advection. Isotopic fractionation during condensation is α_c and during rain evaporation is α_e, which accounts for both equilibrium and kinetic effects. During evaporation from the ocean surface the parameter η accounts for kinetic effects.

Although development of this model is straightforward, the simultaneous inclusion of all terms in the hydrologic balances offers deeper insight to the underlying effects of water cycling on the isotopic composition of atmospheric vapour. This development therefore extends more conventional approaches that consider single processes in isolation, which are derived here as simplifications. Four special cases are considered: (1) only condensation is active (A, E and X are zero), which gives the Rayleigh model; (2) some fraction of the rain is evaporated (A and E are zero), which gives a modified Rayleigh model; (3) only evaporation from the surface is allowed (A, C and X are zero), which gives evaporation mixing lines; and (4) all terms are included but assumed to be at steady state (time derivative set equal to zero). The addition of the advection term tends to dilute the isotopic composition towards the assumed isotope ratio of the advected moisture. These different assumptions lead to different curves in δ–q space (as in Fig. 2) owing to the different degrees to which isotopic fractionation is expressed (detailed descriptions of these models are given in the Supplementary Information). In Fig. 2, cyan curves show Rayleigh distillation to liquid ($\alpha_c \approx 1.105$, solid) and ice ($\alpha_c \approx 1.163$, dashed). The orange curves show evaporation mixing lines that originate from vapour in equilibrium with the ocean surface with given temperature (black curve). The purple dots in Fig. 2c show the steady state model with subsequent modified Rayleigh distillation (purple curves) for the given rain evaporation fraction. Fractionation during rain evaporation of condensate is taken as $\alpha_e = 1.098$ and $\eta = 0.995$.

The rain evaporation fraction can be estimated using the mass balance model by assuming steady state, and solving for f based on the mean tropical values for q_{H_2O} and δD. Specifically, the mass balance is written for cloudy and clear-sky conditions, and assuming the difference between the distributions is due solely to the rain evaporation. The mass balance shows that the isotopic composition of tropospheric vapour over land cannot exceed the isotopic composition of vapour in equilibrium with ocean water unless there is an enriched water source, such as the supply of soil water by evapotranspiration. In the calculation of f, we take $\gamma = 1.157 \times 10^{-5}\,s^{-1}$ and $C = 8\,mm\,day^{-1}$, and A varies from 0 to $8\,mm\,day^{-1}$ given the observed constraints on q_{H_2O} and δ from Fig. 3. For a 12‰ difference between cloudy and clear-sky distributions that share the same isotopic composition near 30° N and 30° S, an f value of 0.2 (20% rain evaporation) is needed to gain balance.

Received 7 February; accepted 30 November 2006.

1. Trenberth, K. E. Changes in tropical clouds and radiation. *Science* **296,** 2095 (2002).
2. Trenberth, K. E., Dai, A. G., Rasmussen, R. M. & Parsons, D. B. The changing character of precipitation. *Bull. Am. Meteorol. Soc.* **84,** 1205–1217 (2003).
3. Roderick, M. L. & Farquhar, G. D. The cause of decreased pan evaporation over the past 50 years. *Science* **298,** 1410–1411 (2002).
4. Bosilovich, M. G., Schubert, S. D. & Walker, G. K. Global changes of the water cycle intensity. *J. Clim.* **18,** 1591–1608 (2005).
5. Emanuel, K. A., Neelin, J. D. & Bretherton, C. S. On large-scale circulations in convecting atmospheres. *Q. J. R. Meteorol. Soc.* **120,** 1111–1143 (1994).
6. Gamache, J. F., Houze, R. A. & Marks, F. D. Dual-aircraft investigation of the inner-core of hurricane Norbert. 3. Water-budget. *J. Atmos. Sci.* **50,** 3221–3243 (1993).
7. Xue, Y. *et al.* Role of land surface processes in South American monsoon development. *J. Clim.* **19,** 741–762 (2006).
8. Dansgaard, W. Stable isotopes in precipitation. *Tellus* **16,** 436–468 (1964).
9. Gat, J. R. Oxygen and hydrogen isotopes in the hydrologic cycle. *Annu. Rev. Earth Planet. Sci.* **24,** 225–262 (1996).
10. Araguas-Araguas, L., Froehlich, K. & Rozanski, K. Deuterium and oxygen-18 isotope composition of precipitation and atmospheric moisture. *Hydrol. Process.* **14,** 1341–1355 (2000).
11. Beer, R., Glavich, T. A. & Rider, D. M. Tropospheric Emission Spectrometer. *Appl. Opt.* **40,** 2356–2367 (2001).
12. Worden, J., Bowman, K. & Noone, D. TES observations of the tropospheric HDO/H_2O ratio: retrieval approach and characterization. *J. Geophys. Res.* **111,** D16309, doi:10.1029/2005JD006606 (2006).
13. Gat, J. R. & Matsui, E. Atmospheric water balance in the Amazon basin: an isotopic evapotranspiration model. *J. Geophys. Res.* **96,** 13179–13188 (1991).
14. Worden, J. *et al.* Predicted errors of tropospheric emission spectrometer nadir retrievals from spectral window selection. *J. Geophys. Res. Atmos.* **109,** D09308, doi:10.1029/2004JD004522 (2004).
15. Hendricks, M. B., DePaolo, D. J. & Cohen, R. C. Space and time variation of $\delta^{18}O$ and δD in precipitation: Can paleotemperature be estimated from ice cores? *Glob. Biogeochem. Cycles* **14,** 851–861 (2000).
16. Schmidt, G. A., Hoffmann, G., Shindell, D. T. & Hu, Y. Modelling atmospheric stable water isotopes and the potential for constraining cloud processes and

stratosphere-troposphere water exchange. *J. Geophys. Res.* **110,** D21314, doi:10.1029/2005JD005790 (2005).
17. Lawrence, J. R. *et al.* Stable isotopic composition of water vapor in the tropics. *J. Geophys. Res. Atmos.* **109,** D06115, doi:10.1029/2003JD004046 (2004).
18. Zhang, G. J. Convective quasi-equilibrium in midlatitude continental environment and its effect on convective parameterization. *J. Geophys. Res. Atmos.* **107,** 4220, doi:10.1029/2001JD001005 (2002).
19. Arakawa, A. & Schubert, W. H. Interaction of a cumulus cloud ensemble with large-scale environment. 1. *J. Atmos. Sci.* **31,** 674–701 (1974).
20. Rosenfeld, D. & Mintz, Y. Evaporation of rain falling from convective clouds as derived from radar measurements. *J. Appl. Meteorol.* **27,** 209–215 (1988).
21. Boville, B. A., Rasch, P. J., Hack, J. J. & McCaa, J. R. Representation of clouds and precipitation processes in the Community Atmosphere Model version 3 (CAM3). *J. Clim.* **19,** 2184–2198 (2006).
22. Gat, J. R. Atmospheric water balance—the isotopic perspective. *Hydrol. Process.* **14,** 1357–1369 (2000).
23. Ehhalt, D. H. *Vertical Profiles of HTO, HDO and H_2O in the Troposphere.* NCAR-TN/STR-100 (National Center for Atmospheric Research, Boulder, 1974).
24. Taylor, A. B. *The Vertical Variations of the Isotopic Concentrations of Tropospheric Water Vapour Over Continental Europe and their Relationship to Tropospheric Structure.* Report INS-R-107 (New Zealand Department of Scientific and Industrial Research, Institute of Nuclear Science, Lower Hutt, 1972).
25. Flanagan, L. B., Comstock, J. P. & Ehleringer, J. R. Comparison of modeled and observed environmental influences on the stable oxygen and hydrogen isotope composition of leaf water in *Phaseolus vulgaris* L. *Plant Physiol.* **96,** 588–596 (1991).

Supplementary Information is linked to the online version of the paper at www.nature.com/nature.

Acknowledgements We thank W. Read, D. Waliser, H. Su, F. Li, E. Fetzer and B. Kahn for discussions on this work, and C. Still, J. Rial and W. Riley for comments on earlier versions of this manuscript. The research described in this paper was carried out at the Jet Propulsion Laboratory, California Institute of Technology, under a contract with the National Aeronautics and Space Administration, and at the University of Colorado.

Author Contributions J.W. and K.B. were responsible for the spectroscopic retrievals of the HDO and H_2O profiles and data quality assurance. D.N. developed the isotopic models and led interpretation of the data. The TES team (see below) helped with the development, analysis and validation of the TES data.

Author Information Reprints and permissions information is available at www.nature.com/reprints. The authors declare no competing financial interests. Correspondence and requests for materials should be addressed to D.N. (david.noone@colorado.edu).

The Tropospheric Emission Spectrometer science team and data contributors: Reinhard Beer[3], Annmarie Eldering[3], Brendan Fisher[3], Michael Gunson[3], Aaron Goldman[4], Robert Herman[3], Susan S. Kulawik[3], Michael Lampel[5], Gregory Osterman[3], Curtis Rinsland[6], Clive Rodgers[7], Stanley Sander[3], Mark Shephard[8], Christopher R. Webster[3] & Helen Worden[3]

Affiliations for participants: [3]Earth and Space Sciences Division, Jet Propulsion Laboratory, 4800 Oak Grove Drive, MS 183-301, Pasadena, California 91109, USA. [4]Department of Physics and Astronomy, University of Denver, Denver, Colorado 80208, USA. [5]Raytheon Company, 299 N. Euclid Avenue, Suite 500, Pasadena, California 91101, USA. [6]NASA Langley Research Center, Hampton, Virginia 23681-0001, USA. [7]Department of Atmospheric Oceanic and Planetary Physics, University of Oxford, Clarendon Laboratory, Parks Road, Oxford OX1 3PU, UK. [8]Atmospheric and Environmental Research Inc. (AER), 131 Hartwell Avenue, Lexington, Massachusetts 02421, USA.